Numerical Heat Transfer, Part A: Applications: An International Journal of Computation and Methodology

TRANSIENT HEAT-TRANSFER PHENOMENON OF TWO-DIMENSIONAL HYPERBOLIC HEAT CONDUCTION PROBLEM

Jhy-Ping Wu [a], Yen-Ping Shu [a] & Hsin-Sen Chu [a]

[a] Department of Mechanical Engineering , National Chiao Tung University , Hsinchu, Taiwan, 300, Republic of China
Published online: 15 Mar 2007.

PLEASE SCROLL DOWN FOR ARTICLE

TRANSIENT HEAT-TRANSFER PHENOMENON OF TWO-DIMENSIONAL HYPERBOLIC HEAT CONDUCTION PROBLEM

Jhy-Ping Wu, Yen-Ping Shu, and Hsin-Sen Chu
Department of Mechanical Engineering, National Chiao Tung University,
Hsinchu, Taiwan 300, Republic of China

This article presents a numerical analysis of the two-dimensional hyperbolic heat conduction problem in an anisotropic medium under a point heat source with different boundary conditions. A simple model has been developed to solve the anisotropic problem. In this analysis, the second-order total variation diminishing (TVD) scheme is employed to solve this problem. The effects of boundary conditions and anisotropy on the thermal wave induced by different types of heat sources in the medium are examined in detail. The results show that the transient behavior of the propagation of the two-dimensional thermal wave is much more complicated than that of the one-dimensional thermal wave due to a circular wave formed to propagate uniformly in all directions, reflections by boundaries, interaction with each other, and serious discontinuity on the wavefront.

INTRODUCTION

The Fourier law of heat conduction, which is the classical theory of diffusion, postulates a heat flux to be directly proportional to a temperature gradient in the form

$$q(r, t) = -k\nabla T(r, t) \tag{1}$$

where k is the thermal conductivity, r the position vector, and t the physical time. According to this law, the traditional heat conduction equation implies an infinite speed of propagation of the thermal wave, indicating that a local change in temperature causes an instantaneous perturbation in the temperature at each point in the medium, even if the intervening distances are large. In other words, heat propagates at an infinite speed, which is incompatible with physical reality. Despite such an unacceptable notion of energy transport in solids, the classical diffusion theory has been widely applied in heat-transfer problems and gives reliable results for most situations encountered in practice, mainly because in most situations the thermal diffusivity is 10 orders of magnitude smaller than that

NOMENCLATURE

$[A], [B]$	Jacobian matrices	T_w	wall temperature
c	speed of thermal wave	$[W]$	eigenmatrix, defined in Eq. (25)
C_p	specific heat	x, y	Cartesian spatial variable
d	length of plate	(x_o, y_o)	position of heat source
e	thermal energy released per	$[Z]$	eigenmatrix, defined in Eq. (27)
	unit length	α	thermal diffusivity, $k/C_p \rho$
E, F	flux vector, defined in Eq. (10)	ε_d	nondimensional thermal energy
F_{01}	nondimensional relaxation time in		released
	x direction, $\tau_x k_y/d^2 \rho C_p$	λ	eigenvalue
F_{02}	nondimensional relaxation time in	ρ	density
	y direction, $\tau_y k_y/d^2 \rho C_p$	τ	relaxation time, α/c^2
g	volumetric energy source		
k	thermal conductivity	**Subscripts**	
K	ratio of thermal conductivity, k_x/k_y		
$[M], [N]$	flux vector, defined in Eqs. (25)	a, b	components for $[A]$ and $[B]$,
	and (29), respectively		respectively
q	heat flux	i, j	control volume index
$\mathbf{q}$	heat flux vector	i or $j \pm \frac{1}{2}$	value at control volume faces
Q	unknown vector, defined in Eq. (10)	r	ratio
$\mathbf{r}$	position vector	x, y	components in x and y directions,
$[R]$	right eigenmatrix, defined in		respectively
	Eq. (15)		
S	source vector, defined in Eq. (10)	**Superscripts**	
t	time		
T	temperature	$n, n + 1$	time levels n and $n + 1$
T_0	initial temperature	$\bar{}$	dimensionless variable
T_{ref}	reference temperature	$[\ ]^{-1}$	inverse matrix

corresponding to the speed of a thermal wave. However, with the advent of science and technology involving very low temperatures near absolute zero, an extremely short transient duration, and an extremely high rate of change of temperature or heat flux, some investigators found that the heat propagation velocity of such situations becomes finite and dominant.

One of the earliest experiments detecting thermal waves was performed by Peshkov [1] using superfluid liquid helium at a temperature of 1.4 K, and the velocity of the thermal wave is 19 m/s. He referred to this phenomenon as "second sound," because of the similarity between the observed thermal waves and ordinary acoustic waves. Von Gutfeld [2] measured the velocity of thermal waves in different dielectric crystals, such as sapphire, GeSi, and NaCl, and their values are all of order 10^3 m/s at low temperature. Maurer and Thompson [3] found that if the surface heat fluxes are greater than on the order of 10^7 W/m^2, the Fourier heat flux model will break down. In recent years, because of the advancement of short-pulse laser technologies and their applications to modern microfabrication technologies, research on high-rate heating on thin film structures has rapidly grown. Human [4] found that the thermal propagation velocity becomes dominant in short-pulse laser heating.

To consider the finite speed of wave propagation, a damped wave model is proposed in the literature by using a variety of reasonings and derivations. Its

development is presented in detail in the review articles by Joseph and Preziosi [5, 6]. Cattaneo [7] and Vernotte [8] independently suggested a modified heat flux model in the form of

$$q(r, t + \tau) = -k\nabla T(r, t) \tag{2}$$

where τ is relaxation time, an intrinsic thermal property of the medium. Equation (2) depicts that the temperature gradient established at time t, due to insufficient response time, results in a heat flux vector at a later time $t + \tau$. This means the heat wave model allows a time lag between the heat flux and the temperature gradient. In fact, the relaxation time τ is associated with the communication "time" between phonons (phonon–phonon collisions) necessary for commencement of heat flow and is a measure of thermal inertia of the medium. Based on the ideas from the collision theory of molecules, τ is approximated to α/c^2 where c is the thermal wave velocity in the medium. Clearly, for $\tau = 0$, Eq. (2) reduces to the classical Fourier law and leads to an infinite propagation velocity. Several investigators [9–12] made attempts to estimate the magnitude of τ for engineering materials. It appears that the magnitude of τ ranges from 10^{-10} s for gases at standard conditions to 10^{-14} s for metals, with values of τ for liquids and insulators falling within this range. Sieniutycz [13] quoted that the τ values for homogeneous substance are of the order 10^{-8} to 10^{-10} s, while recent work by Kaminski [14] on nonhomogeneous inner structure materials revealed values of τ of the order of fractions of a minute. However, for nonhomogeneous materials, Luikov [15] found that the τ values are of the order 10^{-3} to 10^3 s. Recently, Mitra et al. [16] determined experimentally the τ value to be approximately 16 s for biological material and directly validated the hyperbolic nature of heat conduction by comparing experimentally observed temperature with the non-Fourier predictions. Vedavarz et al. [17] have obtained a wide range of τ values for various materials by examining thermophysical property data and using the expressions for relaxation time [10, 11]. The value of this characteristic time is of importance since the conduction processes that occur for time periods of the order of the thermal characteristic time may exhibit significant non-Fourier behavior.

For emphasizing engineering applications of the thermal wave theory, Özisik and Tzou [18] presented a thorough review on thermal wave propagation, which included the sharp wavefront and rate effects, the thermal shock phenomenon, the thermal resonance phenomenon, and reflections and refractions of thermal waves across a material interface. They also employed the dual-phase-lag concept to capture the microscopic mechanisms in some limiting cases. A general criterion for the dominance of wave behavior over diffusion was proposed by Tzou [19]:

$$\frac{\partial T}{\partial t} \gg \left[\frac{T_o c^2}{2\alpha} \exp\left(\frac{c^2 t}{\alpha} \right) \right] \tag{3}$$

with T_o being the reference temperature. According to this criterion, the relative importance of the wave behavior in heat conduction can be examined by considering the interaction of three factors that include the thermal properties (α and c),

the thermal loading and response conditions ($\partial T/\partial t$ and T_o), and the transient time (t). If the heat-transfer process occurs in an extremely short period of time or with an extremely high rate of temperature increase, the wave behavior may become pronounced regardless of the value of T_o. Bai and Lavine [20] have considered the thermodynamic validity of the hyperbolic equations. They proposed a modified hyperbolic-type heat conduction equation that is consistent with the second law of thermodynamic and showed that the conventional hyperbolic heat conduction equation can give physically wrong solutions (temperatures less than absolute zero) under some conditions.

Various analytical and numerical methods [21–28] have been proposed to solve hyperbolic heat conduction problems. However, most problems involving complicated geometries and conditions or variable physical properties must seek the numerical solution. Differing from Fourier heat conduction, where the equations are parabolic, the primary difficulties encountered in hyperbolic heat conduction are concerned mainly with the fictitious numerical oscillations, particularly when sharp propagation fronts and reflective boundaries are involved. Most methods are restricted to analyze one-dimensional frameworks. Recently, there have been two high-resolution numerical schemes [29–30] proposed to solve two-dimensional hyperbolic heat conduction problems. These schemes can effectively reduce the oscillatory magnitudes in the vicinity of the thermal wavefront and successfully reveal the multidimensional reflection and interaction of oblique thermal shocks in complicated geometries. To the best of the authors' knowledge, nobody has focused attention on the thermal wave behavior caused by a single temperature pulse for multidimensional geometry.

The present investigation is concerned with the propagation of a thermal wave in a rectangular plane with the initial point heat source located in an arbitrary position and with anisotropic thermal properties. Two types of heat sources, which are a continuous constant temperature and an instantaneous finite heat flux, are discussed. The boundary conditions on four sides are either adiabatic or a constant wall temperature. We use the second-order total variation diminishing [29] to solve this problem. The results show the complicated reflection and interaction of thermal waves due to heat source and boundary conditions.

PHYSICAL MODEL AND THEORETICAL ANALYSIS

By applying the Taylor series expansion to q in Eq. (2) with respect to τ, and then neglecting the second and higher order terms of τ, the Maxwell–Cattaneo equation or non-Fourier law, the constitutive equation used in the linearized thermal wave theory, can be obtained. Next, combining the non-Fourier law and the constitutive equation and eliminate the heat flux vector leads to the following hyperbolic heat conduction equation with energy sources for the temperature distribution:

$$\frac{1}{c^2}\frac{\partial^2 T}{\partial t^2} + \frac{1}{\alpha}\frac{\partial T}{\partial t} = \nabla^2 T + \frac{1}{k}\left(g + \frac{\alpha}{c^2}\frac{\partial g}{\partial t}\right) \tag{4}$$

where $g(\mathbf{r}, t)$ represents the volumetric energy source in the medium. For the case where $c \to \infty$, Eq. (4) reduces to the classical heat diffusion equation, which corresponds to instantaneous energy diffusion.

In the present investigation, a two-dimensional heat conduction problem in a rectangular plane with constant thermal properties is considered. The thermal conductivity and the velocity of a thermal wave are assumed to be isotropy or anisotropy in the medium. The region is initially in equilibrium at temperature T_0. For times $t > 0$, the surface in the arbitrary situation of the plane is subjected to a point heat source. The types of heat sources are a continuous constant temperature and an instantaneous finite heat flux. Two kinds of boundary conditions, which are the adiabatic and constant wall temperatures, are discussed. The geometry and Cartesian coordinates are depicted in Figure 1. The point heat source is located at an arbitrary location, (x_o, y_o) and extends to infinity normal to the xy plane. Both the width in x direction and the length in y direction of the plane are d.

For convenience in the subsequent analysis, the nondimensionalized variables are defined in the transformed system as follows:

$$\bar{x} = \frac{x}{d}\left(\frac{1}{K}\right)^{1/2} \qquad \bar{y} = \frac{y}{d} \qquad \bar{t} = \frac{k_y t}{d^2 \rho C_p} \qquad (5a)$$

$$\bar{T} = \frac{T - T_o}{T_{ref} - T_o} \qquad \bar{q}_x = \frac{q_x}{k_y(T_{ref} - T_o)/d}\left(\frac{1}{K}\right)^{1/2} \qquad \bar{q}_y = \frac{q_y}{k_y(T_{ref} - T_o)/d} \qquad (5b)$$

where $K = k_x/k_y$, which is the thermal conductivity ratio of x direction to y direction. The energy equation and non-Fourier constitutive equations for the x- and y-direction heat flux components $\bar{q}_x$ and $\bar{q}_y$ are expressed in terms of the preceding dimensionless variables as

$$\frac{\partial \bar{T}}{\partial \bar{t}} + \frac{\partial \bar{q}_x}{\partial \bar{x}} + \frac{\partial \bar{q}_y}{\partial \bar{y}} = 0 \qquad (6)$$
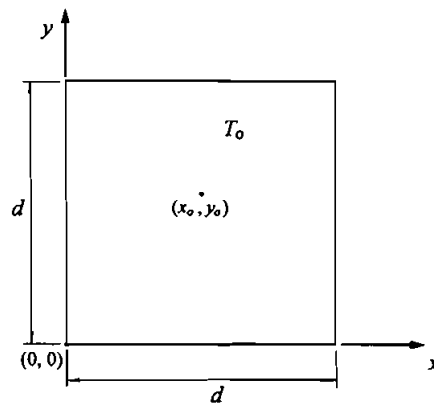

Figure 1. A schematic drawing of a physical model.

$$\frac{\partial \bar{q}_x}{\partial \bar{t}} + \frac{1}{F_{01}} \frac{\partial \bar{T}}{\partial \bar{x}} = -\frac{1}{F_{01}} \bar{q}_x \tag{7a}$$

$$\frac{\partial \bar{q}_y}{\partial \bar{t}} + \frac{1}{F_{02}} \frac{\partial \bar{T}}{\partial \bar{y}} = -\frac{1}{F_{02}} \bar{q}_y \tag{7b}$$

where

$$F_{01} = \frac{\tau_x k_y}{d^2 \rho C_p} \qquad F_{02} = \frac{\tau_y k_y}{d^2 \rho C_p} \tag{8}$$

Equation (6) along with Eq. (7) can be written in dimensionless vector form as

$$\frac{\partial \mathbf{Q}}{\partial \bar{t}} + \frac{\partial \mathbf{E}}{\partial \bar{x}} + \frac{\partial \mathbf{F}}{\partial \bar{y}} = \mathbf{S} \tag{9}$$

$$\mathbf{Q} = \begin{Bmatrix} \bar{T} \\ \bar{q}_x \\ \bar{q}_y \end{Bmatrix} \qquad \mathbf{E} = \begin{Bmatrix} \bar{q}_x \\ \dfrac{1}{F_{01}}\bar{T} \\ 0 \end{Bmatrix} \qquad \mathbf{F} = \begin{Bmatrix} \bar{q}_y \\ 0 \\ \dfrac{1}{F_{02}}\bar{T} \end{Bmatrix} \qquad \mathbf{S} = \begin{Bmatrix} 0 \\ -\dfrac{1}{F_{01}}\bar{q}_x \\ -\dfrac{1}{F_{02}}\bar{q}_y \end{Bmatrix} \tag{10}$$

Equation (9) can be written as

$$\frac{\partial \mathbf{Q}}{\partial \bar{t}} + [A]\frac{\partial \mathbf{Q}}{\partial \bar{x}} + [B]\frac{\partial \mathbf{Q}}{\partial \bar{y}} = \mathbf{S} \tag{11}$$

and the Jacobian matrices are

$$[A] = \frac{\partial \mathbf{E}}{\partial \mathbf{Q}} = \begin{bmatrix} 0 & 1 & 0 \\ \dfrac{1}{F_{01}} & 0 & 0 \\ 0 & 0 & 0 \end{bmatrix} \qquad [B] = \frac{\partial \mathbf{F}}{\partial \mathbf{Q}} = \begin{bmatrix} 0 & 0 & 1 \\ 0 & 0 & 0 \\ \dfrac{1}{F_{02}} & 0 & 0 \end{bmatrix} \tag{12}$$

Then $[A]$ and $[B]$ can be diagonalized through the eigenvectors

$$[A] = [R_a][\lambda_a][R_a]^{-1} \qquad [B] = [R_b][\lambda_b][R_b]^{-1} \tag{13}$$

where $[\lambda_a]$ and $[\lambda_b]$ are the diagonal matrices consisting of three eigenvalues of $[A]$ and $[B]$, respectively. The superscript -1 represents the inverse eigenmatrix.

The diagonal matrices and the right eigenmatrices show that

$$[\lambda_a] = \begin{bmatrix} 0 & 0 & 0 \\ 0 & 1/\sqrt{F_{01}} & 0 \\ 0 & 0 & -1/\sqrt{F_{01}} \end{bmatrix} \quad [\lambda_b] = \begin{bmatrix} 0 & 0 & 0 \\ 0 & 1/\sqrt{F_{02}} & 0 \\ 0 & 0 & -1/\sqrt{F_{02}} \end{bmatrix}$$

(14)

$$[R_a] = \begin{bmatrix} 0 & \sqrt{F_{01}} & \sqrt{F_{01}} \\ 0 & 1 & -1 \\ 1 & 0 & 0 \end{bmatrix} \quad [R_b] = \begin{bmatrix} 0 & \sqrt{F_{02}} & \sqrt{F_{02}} \\ 1 & 0 & 0 \\ 0 & 1 & -1 \end{bmatrix}$$

(15)

In this analysis, the medium is considered to be either isotropic or anisotropic. However, the thermal properties are assumed not to vary with temperature.

Isotropic material: The isotropic thermal properties consist of thermal conductivity and thermal wave velocity in the medium. In other words, these thermal properties are homogeneous and independent of the directions of heat propagation. Then $k_x = k_y$ or $K = 1$ and $F_{01} = F_{02}$. Without loss the generality, we assume $F_{01} = F_{02} = 1$.

Anisotropic material: Thermal waves in anisotropic material, such as ceramic high-temperature superconductors, are much less understood. Various attempts have been made to investigate the heat transfer of anisotropic material concerned with the thermal stability of anisotropic thin-film superconductors. Unfortunately, all the previous research resorts to classical Fourier law [31, 32]. In the present study, we formulate a wave-type heat conduction problem in a rectangular plane with anisotropic thermal properties.

The dimensionless initial conditions are given as

$$\bar{t} = 0 \qquad \begin{cases} \bar{T} = 0 \\ \bar{q}_x = 0 \\ \bar{q}_y = 0 \end{cases}$$

(16)

A three-dimensional analysis would allow the consideration of a release of energy in the form of a finite-length line source, which might be more realistic due to a sudden thermal disturbance, but since the main purpose of this study is to theoretically examine the wave behavior caused by the activation of a pulsed energy source of finite area in multidimensional geometry, a two-dimensional analysis is sufficient. However, a thermal disturbance due to a sudden relaxation of a line dislocation is approximated very well by a line source. Two different types of heat source are discussed as follows:

Instantaneous Finite Heat Flux. At time $\bar{t} = 0^+$, a finite amount of thermal energy ε_d is released in a line source at the location $(\bar{x}_o, \bar{y}_o)$. Immediately after the release of the thermal disturbance, the temperature far away from $(\bar{x}_o, \bar{y}_o)$ is not affected by heat diffusion, and the material transfers no heat to the environment. This leads to an additional initial condition for temperature

$$\int_0^{1/\sqrt{K}} \int_0^1 \bar{T} \, d\bar{x} \, d\bar{y} = \varepsilon_d \qquad \text{for} \quad \bar{t} = 0^+ \tag{17}$$

and a line source is approximated by a deposition of thermal energy in an area $\Delta\bar{x} \, \Delta\bar{y}$ around the point $(\bar{x}_o, \bar{y}_o)$ where

$$\varepsilon_d = \frac{e}{\rho C_p (T_{\text{ref}} - T_o) \sqrt{K} d^2} \tag{18a}$$

$$\bar{T} = \begin{cases} \dfrac{\varepsilon_d}{\Delta\bar{x} \, \Delta\bar{y}} & \bar{x}_o - \Delta\bar{x}/2 \leqslant \bar{x} \leqslant \bar{x}_o + \Delta\bar{x}/2, \; \bar{y}_o - \Delta\bar{y}/2 \leqslant \bar{y} \leqslant \bar{y}_o + \Delta\bar{y}/2 \\ \\ 0 & \text{otherwise} \end{cases}$$

$$\tag{18b}$$

Such an energy source could serve as a model for, for example, application of film/tape superconductors, which is associated with thermal stability under thermal disturbances caused by a sudden relaxation of dislocations, crystal defects, or other spontaneous processes in superconductors [31]. This situation assumes both the film/tape and the disturbance source to be infinite lengths along the current direction, and Figure 1 displays the profile of a cross section normal to the current direction. Another important application concerns a strong or ultra-short-duration laser beam irradiation of absorbing or thin-media surfaces. If the absorbent layer is sufficiently comparable with the thickness of the medium, the energy pulse may be assumed a volumetric source of finite area. Therefore, this physical model can be considered to lump the system in the thickness variable, if the upper and lower surfaces of the plane are also assumed to be adiabatic. In this example, Figure 1 shows the upper surface of plane.

Continuous Constant Temperature. For comparison of the influences of different heat sources on wave behavior, we assume the temperature maintains a constant for all times at the point $(\bar{x}_o, \bar{y}_o)$.

$$\bar{t} > 0 \qquad \bar{T} = T_r \delta(\bar{x} - x_o) \cdot \delta(\bar{y} - y_o) \tag{19}$$

where the dimensionless wall temperature, $T_r = T_w/T_{\text{ref}}$, represents the value of a continuous constant temperature.

The foregoing governing equations, Eqs. (6) and (7), are now considered subject to two kinds of boundary conditions:

Adiabatic:

$$\bar{q}_x(\bar{x} = 0, \bar{y}, \bar{t}) = 0 \qquad \bar{q}_x(\bar{x} = 1, \bar{y}, \bar{t}) = 0 \tag{20a}$$

$$\bar{q}_y(\bar{x}, \bar{y} = 0, \bar{t}) = 0 \quad \bar{q}_y(\bar{x}, \bar{y} = 1, \bar{t}) = 0 \tag{20b}$$

Constant wall temperature:

$$\bar{T}(\bar{x} = 0, \bar{y}, \bar{t}) = 0 \qquad \bar{T}(\bar{x} = 1, \bar{y}, \bar{t}) = 0 \qquad (21a)$$

$$\bar{T}(\bar{x}, \bar{y} = 0, \bar{t}) = 0 \qquad \bar{T}(\bar{x}, \bar{y} = 1, \bar{t}) = 0 \qquad (21b)$$

NUMERICAL METHOD

To solve the system of Eq. (9) for a two-dimensional problem, we use the numerical method developed by Yang [29], which resolves the multidimensional thermal waves without introducing oscillation or dissipation. This method has been validated on one-dimensional and two-dimensional problems before studying this research. Excellent comparisons with analytical results were obtained. For this numerical method, first, Eq. (9) is expanded by both the finite-difference and explicit method. It is assumed that the grid in the computational domain is equally spaced and that the size is unity, so that we have

$$\mathbf{Q}_{i,j}^{n+1} = \mathbf{Q}_{i,j}^{n} - \Delta \bar{t}(\mathbf{E}_{i+1/2,j} - \mathbf{E}_{i-1/2,j}) - \Delta \bar{t}(\mathbf{F}_{i,j+1/2} - \mathbf{F}_{i,j-1/2}) + \Delta \bar{t}\mathbf{S}_{i,j}^{n} \qquad (22)$$

Then by the fractional step (time-splitting) method, which the two-dimensional operator has already split into the product of two one-dimensional operators, we can write Eq. (22) in the form of

$$\mathbf{Q}_{i,j}^{n+1/2} = \mathbf{Q}_{i,j}^{n} - \Delta \bar{t}(\mathbf{E}_{i+1/2,j} - \mathbf{E}_{i-1/2,j}) + \tfrac{1}{2}\Delta \bar{t}\mathbf{S}_{i,j}^{n} \qquad (23a)$$

$$\mathbf{Q}_{i,j}^{n+1} = \mathbf{Q}_{i,j}^{n+1/2} - \Delta \bar{t}(\mathbf{F}_{i,j+1/2} - \mathbf{F}_{i,j-1/2}) + \tfrac{1}{2}\Delta \bar{t}\mathbf{S}_{i,j}^{n+1/2} \qquad (23b)$$

Now it is possible to apply a high-resolution, one-dimensional scheme in each of the preceding steps, and by multiplying Eq. (23a) by $[R_a]^{-1}$, one gets

$$\mathbf{W}_{i,j}^{n+1/2} = \mathbf{W}_{i,j}^{n} - \Delta \bar{t}(\mathbf{M}_{i+1/2,j} - \mathbf{M}_{i-1/2,j}) + \tfrac{1}{2}\Delta \bar{t}\mathbf{S}_{i,j}^{n} \qquad (24)$$

where

$$[W] = [R_a]^{-1} \cdot [Q] \qquad [M] = [\lambda_a] \cdot [W] \qquad [S_a] = [R_a]^{-1} \cdot [S] \qquad (25)$$

Once $[W^{n+1/2}]$ is known, we multiply $[W^{n+1/2}]$ by $[R_a]$ and obtain

$$[Q^{n+1/2}] = [R_a] \cdot [W^{n+1/2}] \qquad (26)$$

The next step is to define

$$[Z^{n+1/2}] = [R_b]^{-1}[Q^{n+1/2}] \qquad [S_b^{n+1/2}] = [R_b]^{-1}[S^{n+1/2}] \qquad (27)$$

and to multiply Eq. (23b) by $[R_b]^{-1}$. Therefore, Eq. (23b) can be transformed to

$$Z_{i,j}^{n+1} = Z_{i,j}^{n+1/2} - \Delta \bar{t}(N_{i,j+1/2} - N_{i,j-1/2}) + \tfrac{1}{2}\Delta \bar{t}S_{b_{i,j}}^{n+1/2} \qquad (28)$$

where

$$[N] = [\lambda_b] \cdot [Z^{n+1/2}] \qquad (29)$$

After $[Z]_{i,j}^{n+1}$ is found, we multiply Eq. (28) by $[R_b]$ to transform $[Q]_{i,j}^{n+1}$. Then, the new values at the time $\bar{t} + 1$ can be fully evaluated.

RESULTS AND DISCUSSION

A two-dimensional computer code was written based on the preceding calculation procedure. Grid refinement studies have also been carried out for the assumed physical model to ensure that the essential physics are independent of grid size. The plane is chosen to be square, with the heat source located at the center of the plane, $(\bar{x}_o, \bar{y}_o) = (0.5, 0.5)$, at $\bar{t} = 0^+$. As in the instantaneous finite heat flux case, the finite amount of thermal energy in a dimensionless type, ε_d, is set 1, which is located over the region $\Delta \bar{x} \Delta \bar{y} = 0.01$ where $\Delta \bar{x} = \Delta \bar{y} = 0.1$. On the other hand, as in the continuous constant temperature case, the value of T_o is assumed to be 1. The present research focuses on the initial transient and on the reflective property of thermal waves for different boundary conditions and heat sources.

Figure 2 shows the temperature profile with the heat source of the continuous constant temperature at different dimensionless time for isotropic material. The distinct wave nature associated with hyperbolic heat conduction dominates. The boundary conditions are adiabatic, which prevents, the heat from transferring through the boundaries and makes, the energy reflect back completely. Again, the initial dimensionless temperature is 0. Clearly, when the temperature at the center at $\bar{t} = 0^+$ is suddenly increased to 1, a circular thermal wave is generated and uniformly propagates to all directions with a constant speed of 1. The results show that for $\bar{t} < 0.5$, in which the thermal wave does not arrive yet at boundaries, an undisturbed region exists ahead of the wavefront due to no molecular communication to occur in Figures 2a and 2b. The magnitude of the discontinuity at the wavefront is attenuated exponentially with time as a result of the diffusion term in the equation. These phenomena, as just mentioned, are similar to those demonstrated in the one-dimensional problems [24].

At $\bar{t} = 0.5$, the wavefront impacts on and reflects from the four insulated boundaries, and then starts to propagate back toward the origin as shown in Figure 2c. Because the boundaries are insulated, heat cannot be absorbed by the environment and the temperature increases at the front after contact. Figure 2d shows that at $\bar{t} = 0.7$ the two reflected thermal waves cross each other on the four corners. This effect induces the temperature to increase double by superposition behind the intersection regions of the reflected waves. Figure 2e can display this effect of positive superposition more clearly. In this figure, the strengthened waves have traveled at a distance from the corners. As time increases, the reflections and

(a) t̄=0.1

(b) t̄=0.3

(c) t̄=0.5

(d) t̄=0.7

(e) t̄=0.9

(f) t̄=1.25

(g) t̄=1.5

(h) t̄=5.0
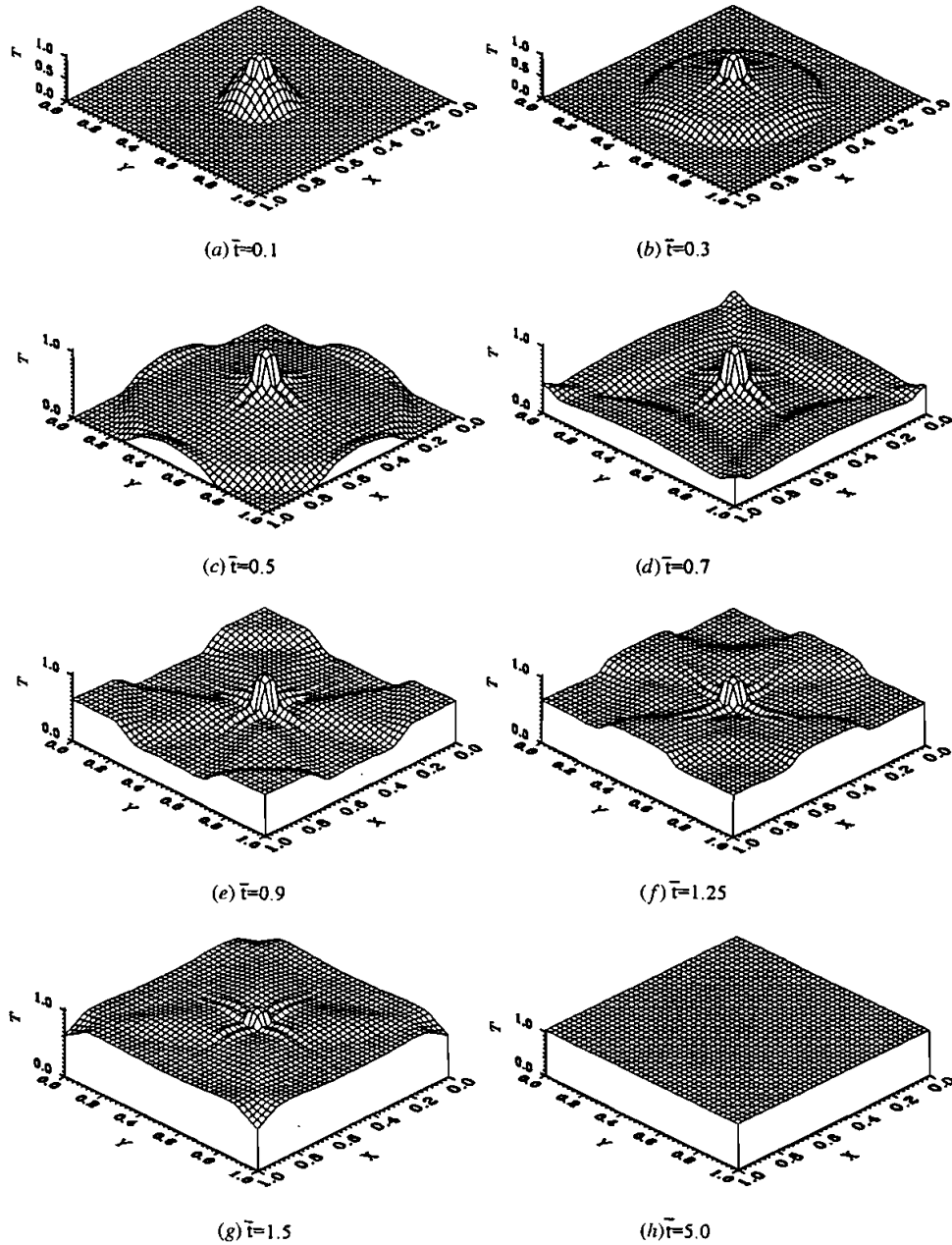
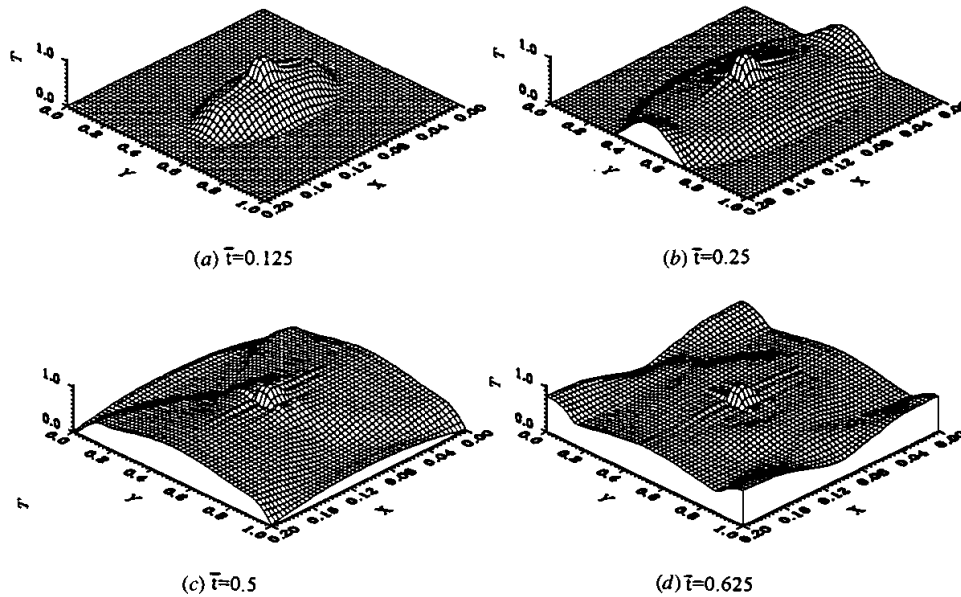**Figure 2.** Temperature profiles in different dimensionless times with the heat source of a continuous constant temperature located at (x_o, y_o) for isotropic medium and constant wall temperature boundaries.

the wave interactions will make the temperature profile in the medium more complex and larger. If the superposition times are different in different situations, the temperature amplitudes can exhibit different values. Clearly, it can been seen that the various temperature values are located at different regions in Figure 2f. When $\bar{t} = 1.5$ in Figure 2g, the temperatures in the whole domain are approaching a uniform value. Until $\bar{t} = 5.0$, the temperature profile display is completely flat and smooth and its value is equal to 1, which is the same as the continuous constant temperature at the center of the plane. In other words, this process of reflections at the boundaries will persist until the diffusion phenomena dominates.

Figure 3 shows the temperature profile of the whole domain at various times (i.e., $\bar{t} = 0.5, 0.7, 0.9, 1.25$) for another case. In this case the physical assumptions are the same as assumed in Figure 2 except the boundary conditions, which are maintained at $\bar{T} = 0$ so that heat can be absorbed by the environment. At any time before the wave encounters the boundaries ($\bar{t} < 0.5$), the behavior of the thermal wave and the temperature profile coincide with the first case in Figure 2, a and b. Equivalently, Figure 3a shows that once the front hits the boundaries, the wave starts to reflect, but the wave moves toward the origin as a reverse-amplitude wave to weaken the positive temperature behind the front. Therefore, a drop in the temperature profile behind the reflected wavefront is generated due to superposition as shown in Figure 3b. Figures 3, c and d, displays the complex temperature profile in the plane due to the boundary reflections and the wave interaction. As time increases, the effect of the wave will gradually decrease until the temperature profile is linear from the origin to the boundaries and axisymmetric around the origin.

(a) $\bar{t}=0.5$ (b) $\bar{t}=0.7$

(c) $\bar{t}=0.9$ (d) $\bar{t}=1.25$
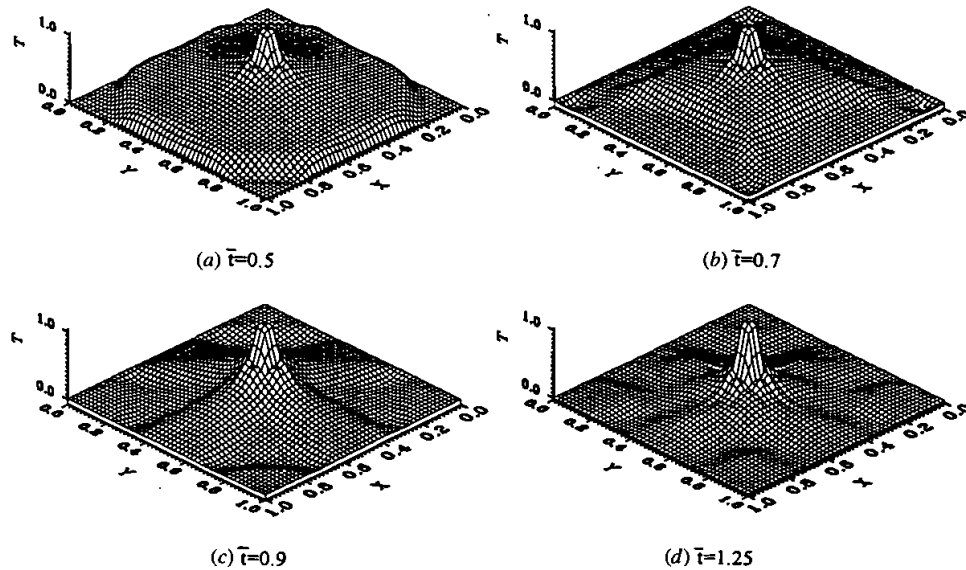
Figure 3. Temperature profiles in different dimensionless times with the heat source of a continuous constant temperature located at (x_o, y_o) for isotropic medium and adiabatic boundaries.

(a) t̄=0.125   (b) t̄=0.25

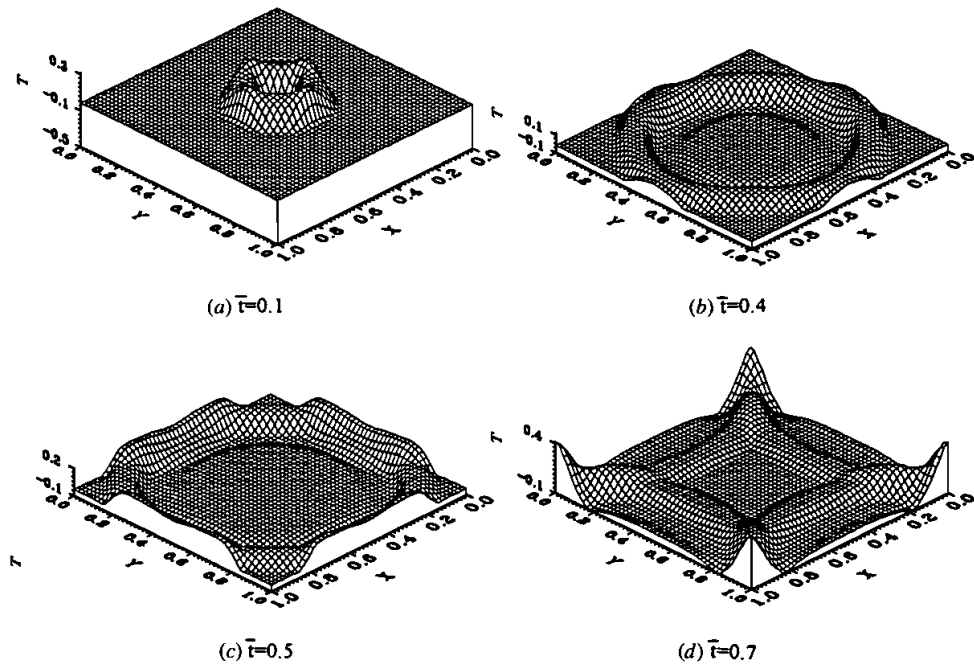(c) t̄=0.5   (d) t̄=0.625

Figure 4. Temperature profiles in different dimensionless times with the heat source of a continuous constant temperature located at (x_0, y_0) for anisotropic medium and adiabatic boundaries.

The evolution of temperature profiles with time for anisotropic thermal properties is shown in Figure 4. The boundary conditions are assumed to be adiabatic, with the dimensionless parameters being $K = k_x/k_y = 25$, $c_r = c_x/c_y = 2$, $F_{01} = 25/4$, and $F_{02} = 1$. Note that the dimensionless widths are 0.2 and 1.0 in the x and y directions, respectively. The wave velocity in the x direction is two times higher than that in the y direction, so the wavefront reaches the boundaries at $\bar{x} = 0$ and 0.2, earlier than the front that reaches the other boundaries in another direction. In this anisotropic case the time to approach a uniform temperature is shorter than that for isotropic material in the previous case, as shown in Figure 3.
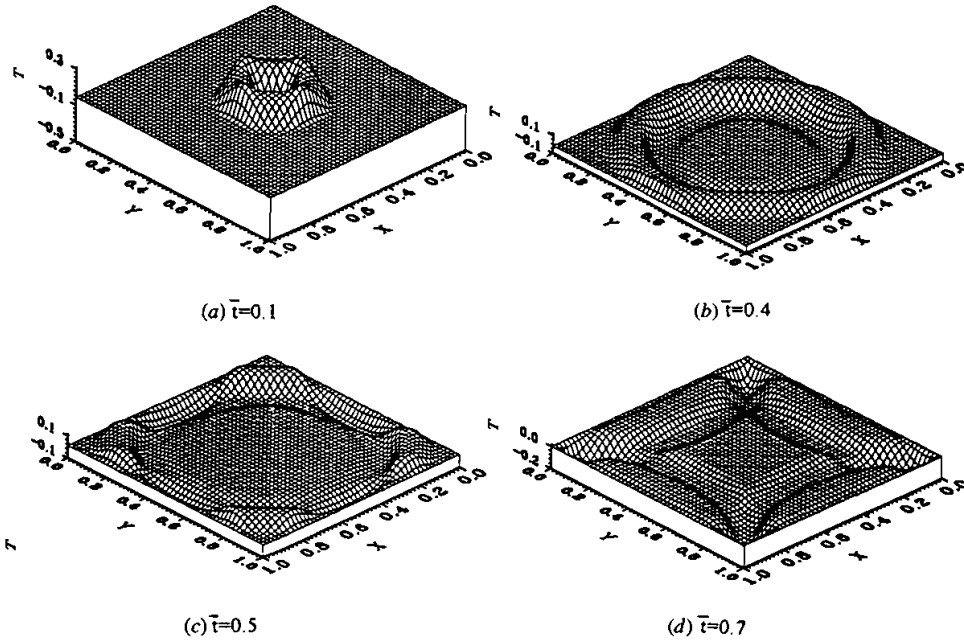
In the instantaneous finite heat flux case, first, we calculate the temperature with adiabatic boundary conditions around the plane. Plots of temperature versus position at various times are presented in Figure 5, with a given pulse area $\Delta \bar{x} \Delta \bar{y} = 0.01$. The results show that an energy pulse gives rise to a thermal wave, which travels in the medium at a finite velocity as in Figure 2 and decays exponentially while dissipating its energy along its path. Note that all energy is concentrated in a wavefront of a finite width, which is preserved for all reflection–transmission effects. The striking feature in Figure 5a, which is different from the results of that of a one-dimension presented by Vick and Özisik [22], is that the negative temperature is generated at the initial time in the vicinity of the origin where the heat source is located. Since a sudden heat pulse induces the heat to accumulate in a wavefront more easily, it thus creates a negative temperature and lulls the strengthened wavefront in order to preserve the energy content of the

(a) t̄=0.1   (b) t̄=0.4

(c) t̄=0.5   (d) t̄=0.7

Figure 5. Temperature profiles in different dimensionless times with the heat source of an instantaneous finite heat flux located at (x_0, y_0) for isotropic medium and adiabatic boundaries.

system. This phenomenon cannot be found in previous research. The negative temperature generated is below the initial temperature. Also, since the external boundaries are insulated for all time $\bar{t} > 0$, the total energy content is constant. As the wave propagates forward, energy is deposited in the wake by diffusion and induces a small but negative residual temperature. At $\bar{t} = 0.4$, the wavefront arrives at the exterior insulated surfaces, and at $\bar{t} = 0.5$, the crest of the wave reaches these surfaces and starts to reflect. When $\bar{t} = 0.7$, the four wavefronts generated by four adiabatic boundaries possess positive amplitude and therefore are directed toward the origin in Figure 5d. Then these fronts begin to cross each other and are strengthened due to the combination at the regions of intersection as seen clearly on the corners. This transmission–reflection combination phenomenon will persist until diffusion dominates. As time increases, the temperature distribution will be smoother and more uniform until the residual temperature approximates an ultimate constant.

The remaining figures help provide a fundamental understanding of the effects of boundary ($\bar{T} = 0$) and anisotropy on hyperbolic heat conduction for instantaneous finite heat flux. Figure 6 shows the effect of the boundary maintained at $\bar{T} = 0$ on temperature distribution. At $\bar{t} = 0.1$, the temperature profile is identical to the graph in Figure 5a since the wavefront is unaware of the boundary effect at this time. The reflected portion, which initially encounters the boundaries at $\bar{t} = 0.4$ and starts to reflect at $\bar{t} = 0.5$, shows a wave moving toward the origin
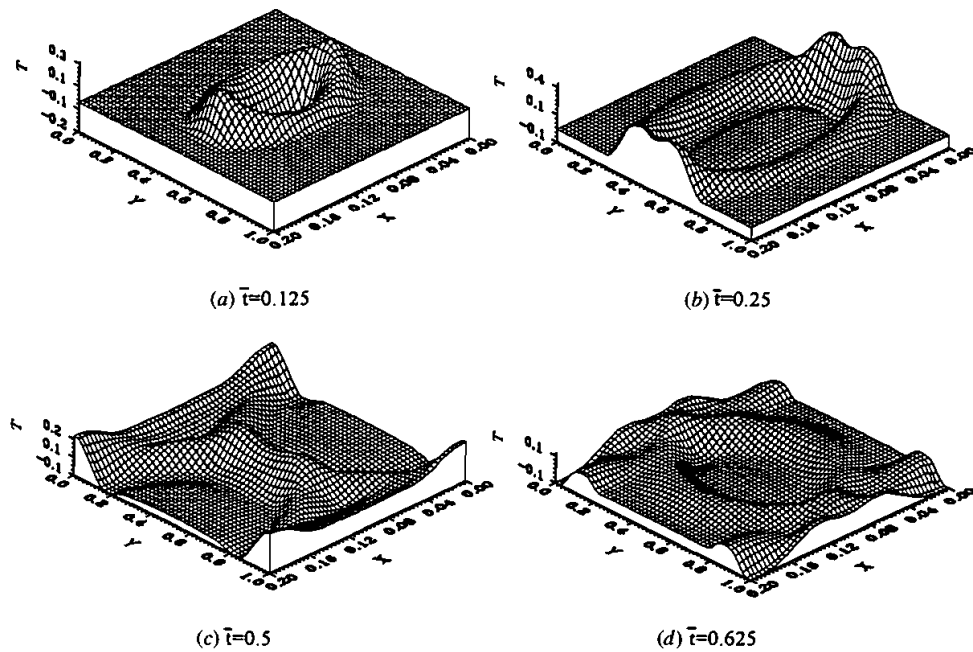
$(a)\,\bar{t}=0.1$ $(b)\,\bar{t}=0.4$

$(c)\,\bar{t}=0.5$ $(d)\,\bar{t}=0.7$

Figure 6. Temperature profiles in different dimensionless times with the heat source of an instantaneous finite heat flux located at (x_0, y_0) for isotropic medium and constant wall temperature boundaries.

but negative in magnitude at $\bar{t} = 0.7$. This negative wavefront is due to the enhanced ability of an environment to transmit energy and the basic criteria of energy conservation. The phenomenon, in which the wavefront is reflected by boundary in different conditions, is analogous with the research for one-dimensional analysis in composite media by Frankel et al. [33]. They reported that internal reflections are produced at the interface of two dissimilar media for a two-region slab exposed to a pulsed volumetric source. The reflected waves in region 1 may be positive or negative in magnitude by judging the thermal conductivity in region 2. The effects of region 2 are similar to that of the environment in our cases. The positive reflected wave due to the adiabatic boundary in our cases can be simulated by assuming the thermal conductivity of region 1 to be lower than that of region 2 in their cases. In contrast, the negative reflected wave due to the boundary at $\bar{T} = 0$ can be simulated by assuming the thermal conductivity of region 1 to be higher than that of region 2.

The effects of isotropy in the medium for adiabatic boundaries are displayed in Figure 7. Since the wave speed ratio is $c_r = c_x/c_y = 2$, we expect double speed in the x direction, as shown clearly in Figure 7a. At $\bar{t} = 0.25$, the wavefront traveling in the x direction is being reflected from the boundaries and the front in another direction arrives only at half of the distance from the origin to the boundary. In Figure 7, c and d, the magnitude of the reflected wave is positive. The transmission-reflection-combination phenomenon is similar to that in Figure 5 but is more complex than that for isotropic materials.

Figure 7. Temperature profiles in different dimensionless times with the heat source of an instantaneous finite heat flux located at (x_o, y_o) for anisotropic medium and adiabatic boundaries.

CONCLUSIONS

A simple model has been developed to solve the two-dimensional anisotropic problem based on hyperbolic heat conduction. The numerical results are presented to display the behavior of the thermal wave for isotropic or anisotropic material with different heat sources, which are a continuous constant temperature and an instantaneous finite heat flux, and the two types of boundary conditions, adiabatic and constant wall temperatures. For a continuous constant temperature, in which the temperature is suddenly increased to a value from the initial temperature and maintains a constant all the time, a discontinuity wavefront is built up and will propagate uniformly toward all directions. In the instantaneous finite heat flux case, an energy pulse located at arbitrary positions induces a circular wavefront of finite width laying on the xy plane, and the wave is positive in magnitude. The interesting feature in this case is that the negative temperature is generated at the initial time around origin. The wavefronts in these cases travel in the medium at a finite velocity and decrease exponentially with time while dissipating their energy along their paths by diffusion. Furthermore, the different boundary conditions may cause a contrary reflected wave. The adiabatic and constant wall temperature boundary produces, respectively, a positive and a negative front. If the material is anisotropic, the transmission−reflection combination phenomenon in a two-dimensional plane is more complex due to different velocity of heat transfer in different

directions. For all cases based on non-Fourier law, as time increases the wave will be reduced until diffusion dominates, and the temperature distribution will be smoother.

REFERENCES

1. V. Peshkov, Second Sound in Helium II, *J. Phys.* USSR, vol. 8, p. 381, 1944.
2. R. J. Von Gutfeld, *Heat Pulse Transmission*, in W. P. Mason (ed.), *Physical Acoustics: Principles and Methods*, chap. 5, Academic Press, New York, 1973.
3. M. J. Maurer and H. A. Thompson, Non-Fourier Effects at High Heat Flux, *ASME J. Heat Transfer*, vol. 95, pp. 284–286, 1973.
4. M. Human, Non-Fourier Heat Transfer in Laser Heated Metal Surfaces, in J. H. Kim et al. (eds.), *Heat Transfer: Korea-U.S.A. Seminar*, pp. 521–533, 1986.
5. D. D. Joseph and L. Preziosi, Heat Waves, *Rev. Modern Phys.*, vol. 61, pp. 41–73, 1989.
6. D. D. Joseph and L. Preziosi, Addendum to the Paper on Heat Waves, *Rev. Modern Phys.*, vol. 62, pp. 375–391, 1990.
7. C. Cattaneo, *Sulla Conduzione De Calore*, Atti del Seminar, Mat. Fis. Univ., Modena, 1948.
8. P. Vernotte, Les Paradoxes de la Theorie Continue de l'Equation de la Chaleur, *C. R. Hebd. Seanc. Acad. Sci.*, Paris, France, vol. 246, pp. 3154–3155, 1958.
9. R. E. Nettleton, Relaxation Theory of Thermal Conduction in Liquids, *Phys. Fluids*, vol. 3, pp. 216–225, 1960.
10. M. Chester, Second Sound in Solid, *Phys. Rev.*, vol. 131, pp. 2013–2015, 1963.
11. M. J. Maurer, Relaxation Model for Heat Conduction in Metals, *J. Appl. Phys.*, vol. 40, pp. 5123–5130, 1969.
12. H. P. Francis, Thermo-Mechanical Effects in Elastic Wave Propagation: A Survey, *J. Sound Vibration*, vol. 21, pp. 181–192, 1972.
13. S. Sieniutycz, The Variational Principles of Classical Type for Non-Coupled Nonstationary Irreversible Transport Processes with Convective Motion and Relaxation, *Int. J. Heat Mass Transfer*, vol. 20, pp. 1221–1231, 1977.
14. W. Kaminski, Hyperbolic Heat Conduction Equation for Materials with a Nonhomogeneous Inner Structure, *ASME J. Heat Transfer*, vol. 112, pp. 555–560, 1990.
15. A. V. Luikov, Application of Irreversible Thermodynamics Methods to Investigation of Heat and Mass Transfer, *Int. J. Heat Mass Transfer*, vol. 9, pp. 139–152, 1966.
16. K. Mitra, S. Kumar, A. Vedavarz, and M. K. Moallemi, Experimental Evidence of Hyperbolic Heat Conduction in Processed Meat, *ASME J. Heat Transfer*, vol. 117, pp. 568–573, 1995.
17. A. Vedavarz, S. Kumar, and M. K. Moallemi, Significance of Non-Fourier Heat Waves in Conduction, *ASME J. Heat Transfer*, vol. 116, pp. 221–224, 1994.
18. M. N. Özisik and D. Y. Tzou, On the Wave Theory in Heat Conduction, *ASME J. Heat Transfer*, vol. 116, pp. 526–535, 1994.
19. D. Y. Tzou, On the Thermal Shock Wave Induced by a Moving Heat Source, *ASME J. Heat Transfer*, vol. 111, pp. 232–238, 1989.
20. C. Bai and A. S. Lavine, On Hyperbolic Heat Conduction and the Second Law of Thermodynamics, *ASME J. Heat Transfer*, vol. 117, pp. 256–263, 1995.
21. K. J. Baumeister and T. D. Hamill, Hyperbolic Heat Conduction Equation: A Solution for the Semi-Infinite Body Problem, *ASME J. Heat Transfer*, vol. 91, pp. 543–548, 1969.
22. B. Vick and M. N. Özisik, Growth and Decay of a Thermal Pulse Predicted by the Hyperbolic Heat Conduction Equation, *ASME J. Heat Transfer*, vol. 105, pp. 902–907, 1983.

23. W. S. Kim, L. G. Hector, Jr., and M. N. Özisik, Hyperbolic Heat Conduction Due to Axisymmetric Continuous or Pulsed Surface Heat Sources, *J. Appl. Phys.*, vol. 68, pp. 5478–5485, 1990.
24. G. F. Carey and M. Tsai, Hyperbolic Heat Transfer with Reflection, *Numer. Heat Transfer*, vol. 5, pp. 309–327, 1982.
25. D. E. Glass, M. N. Özisik, D. S. McRae, and B. Vick, On the Numerical Solution of Hyperbolic Heat Conduction, *Numer. Heat Transfer*, vol. 8, pp. 497–504, 1985.
26. K. K. Tamma and S. B. Railkar, Specially Tailored Transfinite-Element Formulations for Hyperbolic Heat Conduction Involving Non-Fourier Effects, *Numer. Heat Transfer, Part B*, vol. 15, pp. 211–226, 1989.
27. H. Q. Yang, Characteristics-Based, High-Order Accurate and Nonoscillatory Numerical Method for Hyperbolic Heat Conduction, *Numer. Heat Transfer, Part B*, vol. 18, pp. 221–241, 1990.
28. H. T. Chen and J. Y. Lin, Numerical Analysis for Hyperbolic Heat Conduction, *Int. J. Heat Mass Transfer*, vol. 36, pp. 2891–2898, 1993.
29. H. Q. Yang, Solution of Two-Dimensional Hyperbolic Heat Conduction by High-Resolution Numerical Methods, *Numer. Heat Transfer, Part A*, vol. 21, pp. 339–349, 1992.
30. H. T. Chen and J. Y. Lin, Analysis of Two-Dimensional Hyperbolic Heat Conduction Problems, *Int. J. Heat Mass Transfer*, vol. 37, pp. 153–164, 1994.
31. M. I. Flik and C. L. Tien, Intrinsic Thermal Stability of Anisotropic Thin-Film Superconductors, *ASME J. Heat Transfer*, vol. 112, pp. 10–15, 1990.
32. R. C. Chen and H. S. Chu, Study on Intrinsic Thermal Stability of Anisotropic Thin Film Superconductors with a Line Heat Source, *Cryogenics*, vol. 31, pp. 749–755, 1991.
33. J. I. Frankel, B. Vick, and M. N. Özisik, General Formulation and Analysis of Hyperbolic Heat Conduction in Composite Media, *Int. J. Heat Mass Transfer*, vol. 30, pp. 1293–1305, 1987.